arXiv:1212.2745v1 [cond-mat.mtrl-sci] 12 Dec 2012

Giant magnetoimpedance of composite wires with an insulation layer

R. Betzholz,[1, 2] L. Shi,[2] H. Gao,[1] Z. Zhao,[2] and U. Hartmann[1]
[1]*Institute of Experimental Physics, Saarland University,*
P.O. Box 151150, D-66041 Saarbruecken, Germany
[2]*Department of Physics, East China Normal University,*
3663 Zhongshan North Road, 200062 Shanghai, P.R. China

(Dated: December 13, 2012)

Composite wires with a three-layered structure exhibit a large giant magneto-impedance (GMI) effect, which can be used in sensitive magnetic field sensors. To further investigate the origin of the GMI effect, composite wires consisting of a highly conductive copper core, a silicon dioxide layer and an outer Permalloy shell were prepared by radio frequency (RF) magnetron sputtering. The GMI ratio was measured at various driving current frequencies and with different insulating layer thicknesses. A theoretical model by coupling the Maxwell equations to the Landau-Lifschitz-Gilbert equation was developed to investigate the composite wire impedance and its dependence on external magnetic field, current frequency and insulating layer thickness. Experimental results corroborate the theoretical model.

I. INTRODUCTION

The giant magneto-impedance (GMI) effect, initially mentioned as early as in the 1930s,[1,2] gained more interest after the results on nickel-iron alloy microwires were reported in the 1990s.[3–5] The GMI effect refers to the significant change in the impedance Z of a magnetic element with respect to an externally applied static magnetic field. The change of the impedance $\Delta Z/Z$, the so-called GMI ratio, upon the application of a magnetic field is defined as:

$$\frac{\Delta Z}{Z} = \frac{|Z(H)| - |Z(H_{\mathrm{ref}})|}{|Z(H_{\mathrm{ref}})|}, \qquad (1)$$

where H_{ref} denotes a certain reference value of the field, which is chosen to be the maximum applied field strength. $Z = R + iX$ is specified by the resistance R and the reactance X. The relative change of the impedance can easily reach up to several hundred percent and still present a high sensitivity in the low field region of the applied field.[6] Hence the GMI effect has attracted even more attention because of its potential applications as highly sensitive micromagnetic sensors and as read element in magnetic recording.[7–11] The investigation of the GMI effect in low magnetic fields is essential for the enhancement of the sensitivity of the magnetic sensors.[6,12,13] It has been reported that composite-structure materials have a great advantage with respect to the sensitivity in comparison to homogeneous materials,[14–16] especially for composite wires consisting of a highly conductive core and a ferromagnetic shell.[17,18] Furthermore, if an insulation layer is inserted between the core and the shell, the flow of the driving current is restricted to the inner core. It was found that by adding this additional layer, the GMI ratio can be further enhanced.[19–21] To further understand the origin of the giant magneto-impedance effect, especially the GMI ratio enhancement mechanism due to the three-layered structure, composite wires consisting of a highly conductive copper core, a silicon dioxide (SiO_2) layer and an outer Permalloy ($Ni_{80}Fe_{20}$) shell were prepared by radio frequency (RF) magnetron sputtering. GMI ratios were measured at various frequencies and with different insulation layer thickness and the results were analyzed. In order to theoretically model the impedance of the composite wires the distribution of the electric and magnetic field was determined by coupling Maxwell's equations to the Landau-Liftschitz-Gilbert equation and an expression for the permeability in the Permalloy layer was derived.

II. EXPERIMENT

At room temperature, $Ni_{80}Fe_{20}/SiO_2/Cu$ composite wires were prepared by RF magnetron sputtering.[22] Before sputtering, Cu substrate wires with a diameter of 30 μm were firstly immersed into acetone for 30 minutes in order to eliminate the oil attached to the wire surface. After that, they were cleaned using deionized water. Subsequently they were put into a 10% concentrated hydrochloric acid for 30 minutes to remove oxide residues. Finally, the Cu wires were rinsed by deionized water for a second time. The wires were rotated during sputtering process in order to obtain uniform coatings. 40 and 120 revolutions per minute were chosen during the sputtering of SiO_2 and $Ni_{80}Fe_{20}$, respectively. The base vacuum in the sputtering chamber was $2 \cdot 10^{-4}$ Pa. 99.99% pure Ar gas was introduced and kept at a pressure of 0.8 Pa during the deposition of SiO_2 and 0.65 Pa during the deposition of the $Ni_{80}Fe_{20}$ layer. The sputtering power was 230 W for $Ni_{80}Fe_{20}$ with a depositing rate of 12.5 nm/min and 70 W for SiO_2 with a depositing rate of 43.75 nm/min, respectively. The SiO_2 layer thickness was varied to investigate the GMI ratio dependence on the insulation layer thickness. In order to separate Cu and $Ni_{80}Fe_{20}$ completely, both ends of the wires were covered by vulcanized silicone rubber adhesive after the depositing of SiO_2.

The surface morphology and thickness of the coatings were observed and qualified by using SEM. Hysteresis loops were measured by a VSM (Lakershore 7404 model). The wires were exposed to an axial external DC magnetic field generated by a pair of Helmholtz coils. The magneto-impedance (MI) measurements were carried out using HIOKI 3535 LCR and HIOKI 3532 LCR impedance analyzers.

III. THEORETICAL MODELING

The copper core can be defined by its radius r_c and its wire axis which is along the z-axis. Due to the existing of the insulation layer, the driving current $Ie^{-i\omega t}$ with frequency $f = \omega/2\pi$ flows strictly through the copper core. The field distribution can be obtained by solving Maxwell's equations in cylindrical coordinates under neglect of displacement currents.[23] Ampère's law was used as a boundary condition to ensure the restriction of the driving current to the copper core only. The amplitudes E_z of the axial electric field and H_φ of the circumferential magnetic field are represented by functions that solely depend on the radial coordinate r. In CGS units these functions read:[23]

$$E_z(r) = C_1 \frac{J_0(k_c r)}{J_1(k_c r_c)}, \quad H_\varphi(r) = \frac{2I}{c r_c} \frac{J_1(k_c r)}{J_1(k_c r_c)}, \tag{2}$$

with $C_1 = I k_c / 2\pi\sigma_c r_c$, where σ_c denotes the conductivity of the core material copper and c the vacuum speed of light. Furthermore J_n represents Bessel functions of the first kind and order n. k_c is defined by $k_c = (1+i)/\delta_c$, with the skin depth $\delta_c = c/\sqrt{2\pi\omega\sigma_c}$ of the copper core.

No electric current is present in the SiO_2 layer with thickness t_1. The field amplitudes have to satisfy continuity conditions at the conductor-insulator interface. Therefore the solution of Maxwell's equations is then given by

$$E_z(r) = C_2 - C_1 k_c r_c \ln\left(\frac{r}{r_c}\right), \quad H_\varphi(r) = \frac{2I}{cr}, \tag{3}$$

with $C_2 = C_1 J_0(k_c r_c)/J_1(k_c r_c)$. The electric field component E_z consists of a constant and a logarithmically decreasing part, while the magnetic field component H_φ corresponds to the magnetic field of a linear AC conductor.

The solution in the Permalloy shell with thickness t_2 is somewhat more involved, as $\mathbf{B} = \hat{\mu}\mathbf{H}$, with the permeability tensor $\hat{\mu}$. Maxwell's equations that determine the magnetic field component H_φ are now coupled differential equations. As a consequence H_φ and H_z are assumed to be given by series:[25]

$$\begin{aligned} H_\varphi(r) &= C_3 \frac{R}{r} + \sum_n \left(a_n + c_n \ln\left(\frac{r}{R}\right)\right)\left(\frac{r}{R}\right)^n, \\ H_z(r) &= \sum_n \left(b_n + d_n \ln\left(\frac{r}{R}\right)\right)\left(\frac{r}{R}\right)^n. \end{aligned} \tag{4}$$

Here the definition $R = r_c + t_1 + t_2$ was made. These series coincide with the expansions of Bessel functions of the first kind for the decoupled case, in which $\hat{\mu} = \mu\hat{1}$, with the unit tensor $\hat{1}$. Inserting this approach into Maxwell's equations yields recurrence formulae for the sets of coefficients a_n, b_n, c_n and d_n and determines the constant C_3. The electric field components can be derived from H_φ and H_z by using Maxwell's equations for an ohmic conductor with conductivity σ_p, in this case σ_p is the conductivity of Permalloy. Ignoring displacement currents this simplifies to: $\nabla \times \mathbf{H} = 4\pi\sigma_p/c\ \mathbf{E}$. In Eqs. (4), and thereby in the four sets of coefficients, only the three combinations $\mu_\varphi = \mu_{\varphi\varphi} - \mu_{r\varphi}^2/\mu_{rr}$, $\mu_z = \mu_{zz} - \mu_{rz}^2/\mu_{rr}$ and $\mu_c = \mu_{\varphi z} - \mu_{rz}\mu_{r\varphi}/\mu_{rr}$ of the permeability tensor's elements μ_{nm} $(n, m = r, \varphi, z)$ appear. These elements can be obtained by linearizing the Landau-Lifschitz-Gilbert equation[24]

$$\partial_t \mathbf{M}(t) = -\gamma \mathbf{M}(t) \times \mathbf{H}_{\text{eff}} + \frac{\alpha}{M_S} \mathbf{M}(t) \times \partial_t \mathbf{M}(t). \tag{5}$$

This equation describes the dynamics of the magnetization vector $\mathbf{M}(t)$ in the effective magnetic field $\mathbf{H}_{\text{eff}}$. γ denotes the gyromagnetic ratio of the electron, α the Gilbert damping parameter and M_S the saturation magnetization. Linearization was achieved by subdividing the magnetization vector $\mathbf{M}(t)$ and the effective magnetic field $\mathbf{H}_{\text{eff}}$ into their equilibrium parts $\mathbf{M}_{\text{eq}}$ and $\mathbf{H}_{\text{eff}}^{\text{eq}}$ and contributions $\mathbf{M}e^{-i\omega t}$ and $\mathbf{H}e^{-i\omega t}$ that are excited by the driving current.[26] In addition, by using the relation that $\mathbf{M}_{\text{eq}} \times \mathbf{H}_{\text{eff}}^{\text{eq}} = 0$ and by omitting second order terms in the excitation quantities, the Landau-Lifschitz-Gilbert equation can be cast into the form[27,28]

$$\frac{i\omega}{\gamma}\mathbf{M} = \mathbf{M} \times \left(\mathbf{H}_{\text{eff}}^{\text{eq}} + \frac{i\omega\alpha}{\gamma M_S}\mathbf{M}_{\text{eq}}\right) + \mathbf{M}_{\text{eq}} \times \mathbf{H}. \tag{6}$$

This set of equations establishes a linear relation, the susceptibility tensor $\hat{\chi}$, between the magnetization $\mathbf{M}$ and the magnetic field $\mathbf{H}$. The permeability tensor $\hat{\mu}$ can be written as $\hat{\mu} = \hat{1} + 4\pi\hat{\chi}$.

The equilibrium part $\mathbf{H}_{\text{eff}}^{\text{eq}}$ is approximated by the sum of the external field $\mathbf{H}_0$, which is applied in the z direction, and the anisotropy field $\mathbf{H}_k$, which is assumed to be circumferential.[29] The angle ϕ between the equilibrium magnetization and the wire axis is determined by the minimization of the free energy. This results in

$$H_0 \sin(\phi) - H_k \sin(\phi)\cos(\phi) = 0, \tag{7}$$

where H_k is defined by $H_k = 2K_1/M_S$ with the anisotropy constant K_1 for the given material.

Inserting this expression into the permeability tensor yields

$$\begin{aligned} \mu_\varphi &= 1 + \mu_{\text{eff}} \cos^2(\phi)\ , \\ \mu_z &= 1 + \mu_{\text{eff}} \sin^2(\phi)\ , \\ \mu_c &= -\mu_{\text{eff}} \sin(\phi)\cos(\phi)\ . \end{aligned} \tag{8}$$

Here, μ_{eff} plays the role of an effective permeability and μ_φ can be interpreted as the circumferential permeability of the Permalloy shell. For external field strengths sufficiently far above H_K ($\cos(\phi) \approx 1$) the circumferential permeability μ_φ almost equals μ_{eff}. In this case μ_{eff} is defined by

$$\mu_{\text{eff}} = \frac{\omega_M(\omega_M + \omega_k - i\omega\alpha)}{(\omega_M + \omega_k - i\omega\alpha)(\omega_k - i\omega\alpha - \omega_0) - \omega^2} , \qquad (9)$$

with $\omega_M = 4\pi\gamma M_S$, $\omega_k = \gamma H_k$ and $\omega_0 = \gamma H_0 \cos(\phi)$.[30]

Now that the permeability and the field distribution are derived, the impedance of the composite wire can be obtained by considering the energy loss. The input power P is given by $P = ZI^2$. On the other hand the total energy flow dissipated from a volume corresponds to the integral of the Poynting vector $\mathbf{S} = c/4\pi\ \mathbf{E} \times \mathbf{H}$ over its surface. For a composite wire of length l this yields

$$Z = \frac{cl}{2I^2} \sum_{n=1}^{3} (-1)^n r_n \mathbf{E}(r_n) \times \mathbf{H}(r_n) , \qquad (10)$$

with r_n defining the radial coordinates of the three layer surfaces. The impedance Z is a function of the amplitude I and frequency f of the driving current, the wire geometry and additionally, through the permeability tensor, of the applied magnetic field and the anisotropy field.

IV. RESULTS AND DISCUSSION

The above written expression for the impedance allows one to analyze the effect of the applied magnetic field on the impedance and to model the dependence of the GMI ratio on the frequency of the driving current, the wire geometry and the applied field strength. The obtained theoretical predictions can then be compared to experimental findings.

The GMI ratio exhibits a distinct maximum in the vicinity of the value of the anisotropy field.[26] After the applied field exceeds this value, the GMI ratio starts to decrease monotonously. In the case of the Permalloy layer with no magnetic anisotropy this yields a maximum of the GMI ratio in the region of $H_0 = 0$.

Figure 1 depicts the comparison of the theory with experimental results for a sample which exhibits a maximum at $H_0 = 0$. Therefore the parameter H_k in the model was set to zero in this particular case. The wire under investigation was prepared with a SiO_2 thickness $t_1 = 7.2\ \mu$m and a Permalloy layer thickness $t_2 = 8.4\ \mu$m. The parameters for all calculations presented here are $r_c = 30\ \mu$m, $\sigma_c = 5.3 \cdot 10^{17}\ \text{s}^{-1}$, $\sigma_p = 10^{16}\ \text{s}^{-1}$, $c = 3 \cdot 10^{10}\ \text{cm}\,\text{s}^{-1}$, $\gamma = 1.76 \cdot 10^7$, $\alpha = 0.1$, $M_S = 640$ G, $H_{\text{ref}} = 80$ Oe and $I = 10$ mA. For 700 kHz and 1 MHz the model shows a good consistency with the experimental results throughout the whole range of the applied field strength. At higher frequencies, such as 2 MHz in Fig. 1, the comparison shows a discrepancy in the low field region.

Figure 1 also clearly shows that the the driving current frequency has a large influence on the magnitude of the GMI ratio. In order to further investigate the frequency dependence, the theoretical and experimental frequency spectra of the GMI ratio of a composite wire with an insulating layer thickness $t_1 = 7.5\ \mu$m and a Permalloy layer thickness $t_2 = 5.25\ \mu$m are compared in Fig. 2. The comparison shows a good accordance between theory and experiment in a fairly wide frequency range. Below 1 MHz the deviations are smaller than 10%. However, there still is a discrepancy for higher frequencies. The theoretical model delivers results much smaller than the experimental findings above 1 MHz and rapidly drops to zero. This might have its origin in not sufficiently good measurements of the impedance for high frequencies. The fact that the maximum is situated in the region of several hundred kHz is characteristic for composite wires with the given layer structures and has been observed in previous experiments.[20,22]

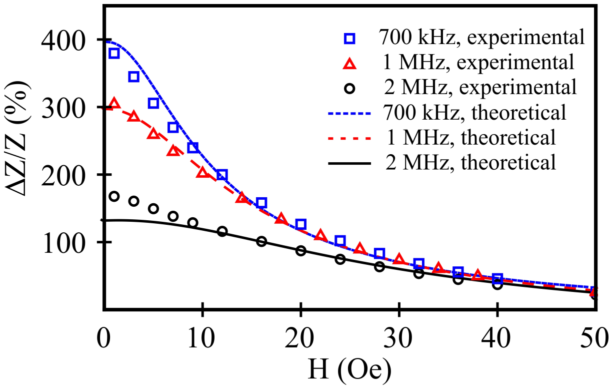

FIG. 1. Comparison of the theoretical model and experimental results for the field dependency of the GMI ratio of a composite wire with an SiO_2 layer thickness of 7.2 μm and a Permalloy shell thickness of 8.4 μm at different frequencies.

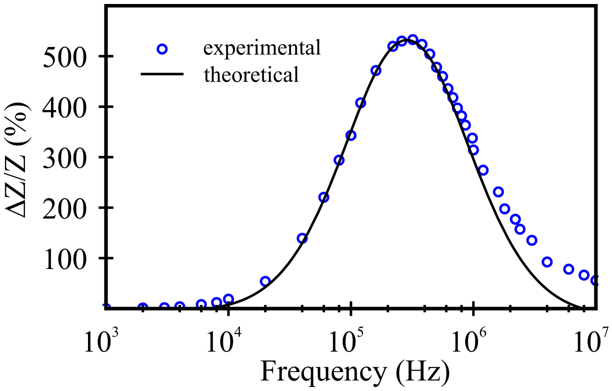

FIG. 2. The frequency spectrum of the GMI ratio of a composite wire with an insulating layer thickness of 7.5 μm and a magnetic shell thickness of 5.25 μm.

Apart from the applied field strength and the driving current frequency the sample geometry has a large impact on the GMI behavior as well. The magnitude of the GMI ratio greatly depends on the thickness t_1 of the insulating layer. Figure 3 represents the analysis of this dependence in the form of frequency spectra for different layer thicknesses. The model predicts a strict decrease of the GMI ratio's peak value for increasing insulation layer thickness, while the experiments show an increase until a certain thickness is reached and only then a decrease for thicker insulating layers. In Fig. 3 the model stays in a fairly good agreement with the experimental data below a frequency of 1 MHz for the insulating layer thicknesses of 5.25 μm and 7.5 μm while there is a considerable disagreement for the composite wire with an insulating layer thickness of only 2.25 μm. This disagreement can be explained by the non uniformity of thin SiO_2 layers on a copper substrate. The non uniformity can reached degrees where even the holes in the layer are present. In that case the insulating effect is of course not given anymore and the driving current will also be distributed in the Permalloy shell, leading to smaller GMI ratios.

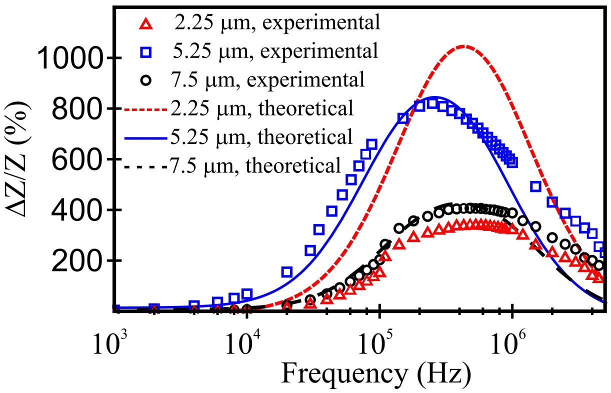

FIG. 3. The frequency spectra of the GMI ratio of composite wires with a magnetic shell thickness of 5.25 μm and different insulating layer thicknesses.

V. CONCLUSION

In conclusion, the expression for the impedance of composite wires with insulating layer was derived by separately solving Maxwell's equations in every layer under usage of boundary conditions that restrict the flow of the driving current to the copper core, linearizing the Landau-Lifschitz-Gilbert equation to obtain the permeability tensor and finally considering the energy loss. Due to the linerarization of the Landau-Lifschitz-Gilbert equation and the disregard of terms in the effective magnetic field the permeability expression is based on several approximations. Nevertheless, experimental results corroborate the theoretical model of the field dependence of the GMI ratio. Furthermore, the frequency dependence is predicted quite accurately up to a certain frequency. The reason for the discrepancies in both dependencies might be attributed to the simplifications made in the derivation of the model and inaccuracies in the measurements. The analysis of the insulating layer thickness' influence on the GMI behavior showed a strong disagreement with experimental outcomes for thin layer thicknesses. In the model the trend of the maximum in the frequency spectrum is only consistent with experiments for insulating layers thicker than a certain value. This can be explained by the non-uniformity of thin silicon dioxide layers on a copper wire substrate.[21] Thin layers can exhibit holes that constitute an electric contact between the copper core and the outer Permalloy shell, thus removing the restriction of the driving current to the copper core and making the boundary conditions used in the model inapplicable. Therefore the GMI ratio of composite wires could be increased by depositing insulating layers with high degrees of uniformity and small thicknesses.

---

[1] E. P. Harrison, G. L. Turney, and H. Rowe, Nature **135**, 961 (1935)

[2] E. P. Harrison, G. L. Turney, H. Rowe, and H. Gallop, Proc. R. Soc. Lond. A **157**, 451 (1936)

[3] L. V. Panina and K. Mohri, Appl. Phys. Lett. **65**, 1189 (1994)

[4] R. S. Beach and A. E. Berkowitz, Appl. Phys. Lett. **64**, 3652 (1994)

[5] L. V. Panina, K. Mohri, T. Uchiyama, M. Noda, and K. Bushida, IEEE Trans. Magn. **31**, 1249 (1995)

[6] M. Vázquez, J. Magn. Magn. Mater. **226**, 693 (2001)

[7] L.V. Panina and K. Mohri, J. Magn. Soc. Jpn. **18**, 245 (1994).

[8] S. Yoon, P. Kollu, D. Kim, G. Kim, Y. Cha, and C. Kim, IEEE Trans. Magn. **45**, 2727 (2009)

[9] A. Zhukov, M. Ipatov, and V. Zhukova, J. Optoelectron. Adv. Mater. **14**, 309 (2012)

[10] S. Corodeanu, T.-A. Ovari, N. Lupu, and H. Chiriac, IEEE Trans. Magn. **46**, 380 (2010)

[11] G. Yu, X. Bu, B. Yang, Y. Li, and C. Xiang, IEEE Sensors J. **11**, 2273 (2011)

[12] W. Zhao, X. Bu, G. Yu, and C. Xiang, J. Magn. Magn. Mater. **324**, 3073 (2012)

[13] M. Langosch, H. Gao, and U. Hartmann, J. Phys. D: Appl. Phys. **45**, 085001 (2012)

[14] L.V. Panina, K. Mohri, and T. Uchiyama, Physica A **241**, 429 (1997)

[15] S. Q. Xiao, Y. H. Liu, S. S. Yan, Y. Y. Dai, L. Zhang, and L. M. Mei, Phys. Rev. B **61**, 5734 (2000)

[16] V. Zhukova, M. Ipatov, A. Zhukov, J. Gonzalez, and J. M. Blanco, Sens. Act. B-Chem **126**, 232 (2007)

[17] H. L. Seet, X. P. Li, Z. J. Zhao, L. C. Wong, H. M. Zheng, and K. S. Lee, J. Magn. Magn. Mater. **302**, 113 (2006)

[18] L. P. Liu, Z. J. Zhao, J. C. Zhang, Z. M. Wu, J. Z. Ruan, Q. J. Wang, and X. L. Yang, J. Magn. Magn. Mater. **305**, 212 (2006)

[19] X. Z. Wang, W. Z. Yuan, X. D. Li, J. Z. Ruan, Z. J. Zhao, J. X. Yang, X. L. Yang, and Z. Sun,

J. Magn. Magn. Mater. **308**, 269 (2007)

[20] J. K. Cheng, Z. J. Zhao, H. Lin, Z. M. Wu, X. L. Yang, and W. Z. Yuan, J. Magn. Magn. Mater. **320**, 994 (2008)

[21] L. Shi, J. Ruan, J. Zhang, Z. Zhao, H. B. Gao, and U. Hartmann, Physica B **404**, 3766 (2009)

[22] Q. Zhang, Q. Mao, J. Ruan, Q. Wang, X. Yang, and Z. Zhao, J. Magn. Magn. Mater. **320**, 2319 (2008)

[23] L. D. Landau and J. M. Lifschitz, *Electrodynamics of Continuous Media* (Pergamon, Oxford, 1990)

[24] T. L. Gilbert, IEEE Trans. Magn. **40**, 3443 (2004)

[25] N. A. Buznikov, A. S. Antonov, A. B. Granovsky, C. G. Kim, C. O. Kim, X. P. Li, and S. S. Yoon, J. Magn. Magn. Mater. **296**, 77 (2006)

[26] M. Knobel, M. Vázquez, and L. Kraus, Handbook of Magnetic Materials **15**, 497 (2003)

[27] G. Bertotti, *Hysteresis in Magnetism* (Academic Press, New York, 1998)

[28] L. Kraus, G. Infante, Z. Frait, and M. Vázquez, Phys. Rev. B **83**, 174438 (2011)

[29] D. P. Makhnovskiy, L. V. Panina, and D. J. Mapps, Phys. Rev. B **63**, 144424 (2001)

[30] N. A. Usov, A. S. Antonov, and A. N. Lagar'kov, J. Magn. Magn. Mater. **185**, 159 (1998)